Modelisation of the contribution of the Na/Ca exchanger to cell membrane potential and intracellular ion concentrations

S. Bahlouli, F. Hamdache and H. Riane

Laboratoire de Physique des Plasmas, Matériaux Conducteurs et leurs Applications, Département de Physique, USTO'MB, BP 1505, Al Menouer Oran, Algeria

Abstract. Modelisation plays a significant role in the study of ion transfer through the cell membrane and in the comprehension of cellular excitability. We were interested in the selective ion transfers through the K_{Ca}, Na_v, Ca_v channels and the Na/Ca exchanger (NCX). The membrane behaves like an electric circuit because of the existence of ion gradients maintained by the cell. The non-linearity of this circuit gives rise to complex oscillations of the membrane potential. By application of the finite difference method (FDM) and the concept of percolation we studied the role of the NCX in the regulation of the intracellular Ca^{2+} concentration and the oscillations of the membrane potential. The fractal representation of the distribution of active channels allows us to follow the diffusion of intracellular Ca^{2+} ions. These calculations show that the hyperpolarization and the change in the burst duration of the membrane potential are primarily due to the NCX.

Key words: Percolation — Finite difference method — Ion channels and concentrations — Current clamp — Voltage clamp

Introduction

The plasma membrane constitutes a selective barrier between the inside and the outside of a cell. It controls the entry and the exit of various molecules and ions between the two compartments. All cells develop a potential difference (PD) between the two faces of the membrane. This PD is responsible for the electric activity of excitable cells, which appears in the form of oscillations of the membrane potential. These oscillations take place in many physiological processes, in particular in neuronal, cardiac and pancreatic cells (Wakimoto et al. 2000; Barg et al. 2001; Munekazu and Iwamoto 2001; Bano et al. 2005).

The aim of this work was to evaluate the role of a membrane protein, the Na/Ca exchanger (NCX) in the regulation of the oscillations of the membrane potential. NCX allows Ca^{2+} extrusion from the cell and entry of Na^+ along its electrochemical gradient without energy consumption. In addition, because NCX is electrogenic and voltage dependent, it can reverse dur-

ing cellular activation and contributes to Ca^{2+} entry into the cell (Blaustein and Lederer 1999). In β-cells and the heart, NCX seems to be the predominant mechanism for Ca^{2+} extrusion, accounting for approximately 70 and 90% of Ca^{2+} extrusion, respectively (Bers et al. 1996; Van Eylen et al. 1998).

We used the percolation concept introduced in 1953 by Hammersley in order to describe statistical systems made up of a great number of objects which can be connected between them. According to the number of objects put in contact, the long-range communication is either possible or non-existent. Between the two modes of communication, there is a threshold of precise transition, called percolation threshold (Stauffer and Aharony 1991). The critical behaviour of the system in the vicinity of this threshold is characteristic of a phase transition.

In the case of biological systems, the research of the transport properties is a complex problem due to its mathematical aspect. It is more judicious to study the biological systems by modelling them on simple networks. By using the two-dimensional networks, we can simulate many systems and have very approximate values of the parameters, which characterise them.

The first computational model of the action potential (AP) was formulated by Hodgkin and Huxley for the

Correspondence to: Samia Bahlouli, Laboratoire de Physique des Plasmas, Matériaux Conducteurs et leurs Applications, Département de Physique, USTO'MB, BP 1505, Al Menouer Oran, Algeria
E-mail: ba_samia@hotmail.com

axon (Hodgkin 1948; Hodgkin and Huxley 1952). Their circuit model of the cell membrane remains the basis for modern AP models. In this case, we modelled the transfer of ions through channels of a cellular membrane by using a square electrical network of conductances randomly distributed, which represent three different channels: the potassium channels (K_{Ca}), activated by intracellular Ca^{2+}, the voltage-gated sodium channels (Na_v) and the voltage gated calcium channels (Ca_v). The fuses are connected in series with the conductances to highlight the activation and the inactivation of channels. The dielectric property of the phospholipids is represented by a capacity in parallel with the network. The phase transition of the system is described by the change in the vicinity of the percolation threshold from the non-permeability to the permeability of the membrane.

Our goal was to study the diffusion of ions through the membrane. For that, we have to use the Fick's laws, which treat partial derivative equations. Analytically, the solution of these equations is very difficult and sometimes impossible. We used a very simple numerical method – the finite difference method (FDM) (Garrido et al. 1985; Morton and Mayers 1995; Miloshevsky et al. 2006) in order to find the concentrations at each node of the network. FDM proceeds by replacing the derivatives of the differential equations by finite difference approximations. This gives a large algebraic system of equations, which can be solved in place of the differential equations.

We used to simulate two measurement techniques: the current-clamp (Hilgemann 1988; Zhan et al. 1999; Dallas et al. 2008) and the voltage-clamp (González-Caballero et al. 1988; Leois and Rae 1998) for better including the ion mechanisms. This model enabled us to study the effect of NCX on the membrane potential and the change in intracellular Ca^{2+} concentration.

Ion transfer and FDM

In our simulation, we have to solve partial derivative equations. For that, it is necessary to use a numerical method of resolution, we chose FDM for its mathematical and data-processing simplicity.

The transfer of the ions through the channels is a nonstationary electrochemical diffusion (Bergamini et al. 1998). We consider the regular mesh of field Ω represented in Fig. 1. We study a problem of advection diffusion (Hundsdorfer and Verwer 2003; El Makrini et al. 2007) characterised by a uniform transport velocity v according to the x direction and the diffusion coefficients D_α ($\alpha = K^+, Na^+, Ca^{2+}$, constant for each ion).

The equation controlling the ion transport is given by the Fick's 2nd law (Flynn 1972; Flynn et al. 1974; Rappaz et al. 1998):
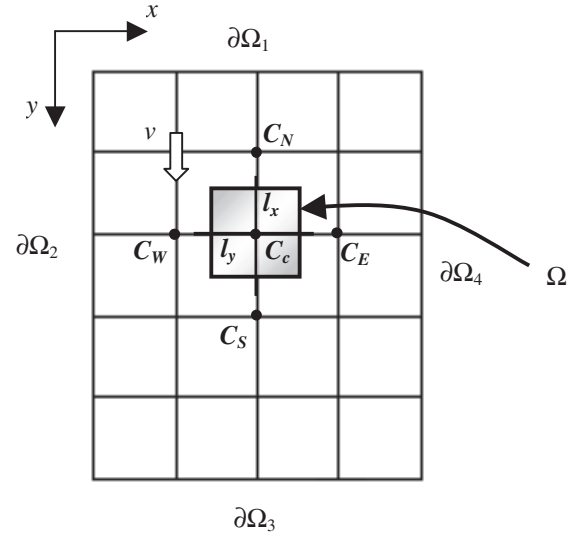
Figure 1. Representation of the regular mesh of field Ω of dimension $lx = ly = l$. E (East), W (West), N (North), S (South) are the neighbours of the central node C.

$$\frac{\partial C_\alpha}{\partial t} - D_\alpha \mathrm{div}(\mathrm{grad}C_\alpha) + v\,\mathrm{grad}C_\alpha = \frac{\partial C_\alpha}{\partial t} -.$$

$$- D_\alpha[\frac{\partial^2 C_\alpha}{\partial x^2} + \frac{\partial 2 C_\alpha}{\partial y^2}] + v\frac{\partial C_\alpha}{\partial x} = 0 \tag{1}$$

With $C_\alpha(x,y,t)$ are the concentrations of K^+, Na^+, Ca^{2+}, respectively.

To solve this equation, we take account of the boundary conditions on the four borders (Rappaz et al. 1998):

$$\partial\Omega_1 : C_\alpha(x,t) = \tilde{C}_\alpha \qquad \text{(Dirichlet condition)} \tag{2}$$

$$\partial\Omega_2 : D\frac{\partial C_\alpha}{\partial n} = -D\frac{\partial C_\alpha}{\partial y} = q \quad \begin{array}{l}\text{(Neumann condition,}\\ \text{imposed flow)}\end{array} \tag{3}$$

$$\partial\Omega_3 : D\frac{\partial C_\alpha}{\partial n} = -D\frac{\partial C_\alpha}{\partial x} = 0 \quad \begin{array}{l}\text{(homogeneous}\\ \text{Neumann condition)}\end{array} \tag{4}$$

$$\partial\Omega_4 : D\frac{\partial C_\alpha}{\partial n} = -D\frac{\partial C_\alpha}{\partial y} = -\beta(C_\alpha - \tilde{C}_a) \quad \begin{array}{l}\text{(Cauchy}\\ \text{condition)}\end{array} \tag{5}$$

To apply the FDM, the rectangular field of dimension $lx = ly = l$ is squared according to the axes directions as illustrated in Fig. 1. The neighbours of a central node of index C are located by the letters E (east), W (west), N (north), S (south). If the neighbour exists, we call h the distance separating it from the central node.

By using the Taylor's series expansions and the FDM at the node C, the Eq. (1) becomes:

$$\frac{1}{F_{Oh}}(C_{\alpha c}{}^{j+1} - C_{\alpha c}{}^{j}) - (C_{\alpha E} + C_{\alpha W} + C_{\alpha N} + C_{\alpha S} - 4C_{\alpha C})^{\theta} +$$

$$+ \frac{P_{eh}}{2}(C_{\alpha E} - C_{\alpha W})^{\theta} = 0 \qquad (6)$$

The linear combinations of the Eq. (6) are indexed with θ to separate the explicit and implicit finite difference forms. P_{eh} is a Péclet number: $P_{eh} = (v \cdot h)/D$, F_{Oh} is a Fourier number: $F_{Oh} = (D \cdot \Delta t)/h^2$.

By using the Courant, Friedricks and Levy condition (CFL) which is $D \cdot \Delta t/h^2 \le 1/4$ at $v \cdot h/D \le 1/2$, we impose the stability criteria $F_{Oh} \le 1/4$ at $P_{eh} \le 2$ (Strikwerda 1989; Rappaz et al. 1998).

The model

We keep the same structure of grid like the FDM and we use a square network of size L. The conductive ion channels are characterised by their elementary conductance: γ_{K-Ca}, γ_{Na}, γ_{Ca} randomly distributed with open probability: P_{K-Ca}, P_{Na}, and P_{Ca}, and with intracellular ion concentrations C_{K-Ca}, C_{Na} and C_{Ca}, respectively. The probability of opening and closing of ion channels is represented by a fuse connected in series with the conductances. The dielectric character of the double-layer of lipid is represented by a capacity C_m (Fig. 2).

We chose three types of ion channels:
- The potassium channels (K_{Ca}), activated by intracellular Ca^{2+} (Romero et al. 1998; Siwy et al. 2001; Ledoux et al. 2006; Zhao et al. 2007), named BK or maxi-K slightly sensitive to the variations of the membrane potential whose conductance varies between 180 and 300 pS.
- The voltage-gated sodium channels (Na_v), responsible of the ascending phase of the action potential (Stuart and Hausser 1994; Hollerbach et al. 2000), with a conductance of 10–15 pS.
- The voltage gated calcium channels (Ca_v) whose conductance varies between 11 and 20 pS (Nonner and Eisenberg 1998; Boda et al. 2004; Elbasiouny et al. 2005).

The current through a selective channel is given by the Ohm's law and the Nernst equation (Hille 2001). We apply to the circuit the first Kirchhoff law:

$$C_m \frac{dV}{dt} = -I_{ion}(V) \qquad (7)$$

In our model, the total current (I_{ion}) is the sum of three currents: I_{Na} which represents the depolarizing Na^+ current, I_{K-Ca} that accounts for the hyperpolarizing K^+ current and the slowly activating Ca^{2+} current I_{Ca}. We shall assume for simplicity that: i) the relaxation kinetics are first order (Milescu et al. 2005; Rudy and Silva 2006) and described by any time homogeneous Markov process (Goldman 1991; Venkataramanan and Sigworth 2002; Faber et al. 2007), in which the channel jumps from the open state to the closed state; ii) the time constants of the Ca^{2+} and Na^+ current are small compared to the potential bursting, for that we use the measured values for parameters and theoretical expressions for activation levels given by Rorsman (Rorsman and Trube 1986) and Sherman (Sherman et al. 1988).

These currents are given according to the Hodgkin-Huxley (Hodgkin and Huxley 1952) and Morris-Lecar models (Morris and Lecar 1981; Rinzel and Ermentrout 1999), and have the following expressions:

$$I_{Na} = \gamma_{Na} \cdot m^3 \cdot h \cdot (V_m - E_{Na}) \qquad (8)$$

$$I_{K-Ca} = \gamma_{K-Ca} \cdot z \cdot (V_m - E_K) \qquad (9)$$
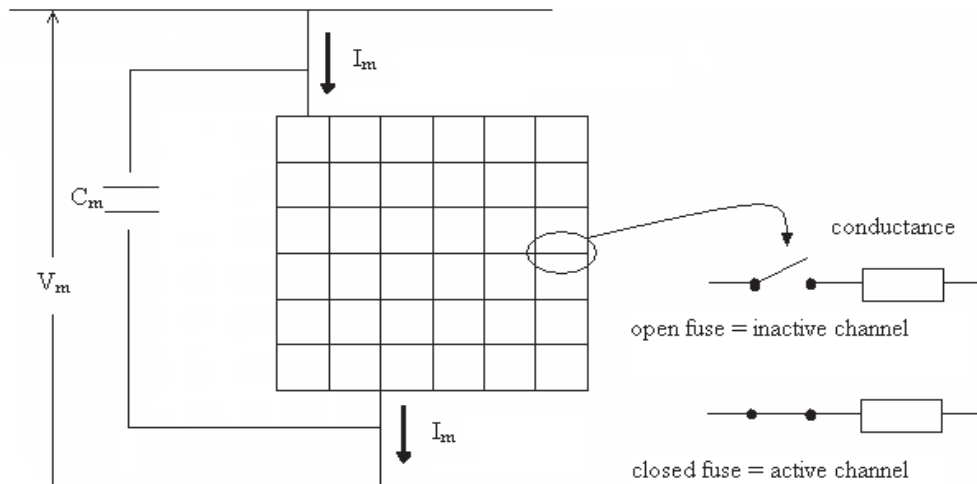
Figure 2. Schematization of the square network of size 6×6 of conductances and fuses randomly distributed.

$$I_{Ca} = \gamma_{Ca} \cdot m \cdot h \cdot (V_m - E_{Ca}) \tag{10}$$

where: E_{Na}, E_K and E_{Ca} are the reversal potentials (in mV) and m is the open probability of the activation gate, described by

$$m = \frac{1}{1 + \exp[(4 - V)/14]} \tag{11}$$

h is the open probability of a single first-order inactivation gate, given by the sigmoidal function:

$$h = \frac{1}{1 + \exp[(V + 10)/10]} \tag{12}$$

z is the gating variable with a Hill-like dependence on C_{Ca}

$$z = \frac{C_{Ca}}{C_{Ca} + 1} \tag{13}$$

and the balance equation for C_{Ca} is:

$$\frac{dC_{Ca}}{dt} = 0.005(-0.2 \cdot I_{Ca} - C_{Ca}) \tag{14}$$

The FDM imposes known concentrations on the four edges of the circuit. We chose the potassium concentrations $C_{K\text{-}Ca}$ because, at rest, the membrane is essentially permeable to potassium.

Results and Discussion

In our model, the elementary conductances are: $\gamma_K = 200$ pS, $\gamma_{Na} = 12$ pS and $\gamma_{Ca} = 15$ pS. The membrane capacity per unit of area of the biological membranes is: $C_m = 1$ µF/cm².

The intracellular concentrations have values higher or equal to physiological values such as: $C_{K\text{-}Ca} = 100$ mmol/l, $C_{Na} = 10$ mmol/l and $C_{Ca} = 1$ µmol/l. The extracellular concentrations will not be modified and correspond to the physiological values (Hille 2001).

Since the studied problem is a pure diffusion, the numbers of Fourrier and Péclet are $F_{Oh} = 1/2$ and $P_{eh} = 1$ (Phannkuch 1963; Muradoglu and Tryggvason 2008).

To solve the differential Eqs. (7) and (14) we used the numerical algorithms group library of Fortran and the D02BBF subroutine (Ermentrout 2003; Metcalf et al. 2004).

The direction of the ion flows, the gradients of concentration and the variations of membrane potential are controlled for any iteration. The results are obtained after 1000 iterations.

Percolation threshold

In a random system, the transport phenomena are studied in the vicinity of the percolation threshold. We have to find the threshold probability for which the membrane forwards

impermeable phase (non-conducting) to the permeable phase (conducting).

We varied the probabilities P_K, P_{Na} and P_{Ca} from 0 to 1, for the intracellular concentrations $C_{K\text{-}Ca} = 140$ mmol/l, $C_{Na} = 20$ mmol/l and $C_{Ca} = 1$ µmol/l. For each probability, we calculated the membrane conductance by the star-triangle transformation, in order to reduce the matrix size from $[L^2 \times L^2]$ to $[L \times (L + 1)]$:

$$v_e^{(\chi)}(i,j) = [h_o(i,j)^{(\chi-1)} \times v_e^{(\chi-1)}(i,j) + v_e^{(\chi-1)}(i+1,j) \times$$
$$\times v_e^{(\chi-1)}(i,j) + v_e^{(\chi-1)}(i+1,j) \times h_o^{(\chi-1)}(i,j)] / v_e^{(\chi-1)}(i,j) \tag{9}$$

$$v_e^{(\chi)}(i+1,j) = [h_o(i,j)^{(\chi-1)} \times v_e^{(\chi-1)}(i,j) + v_e^{(\chi-1)}(i+1,j) \times$$
$$\times v_e^{(\chi-1)}(i,j) + v_e^{(\chi-1)}(i+1,j) \times h_o^{(\chi-1)}(i,j)] / h_o^{(\chi-1)}(i,j) \tag{10}$$

$$h_o^{(\chi)}(i,j) = [h_o(i,j)^{(\chi-1)} \times v_e^{(\chi-1)}(i,j) + v_e^{(\chi-1)}(i+1,j) \times$$
$$\times v_e^{(\chi-1)}(i,j) + v_e^{(\chi-1)}(i+1,j) \times h_o^{(\chi-1)}(i,j)] / v_e^{(\chi-1)}(i+1,j) \tag{11}$$

Where $v_e(i,j)$ and $h_o(i,j)$ represent vertical and horizontal conductances respectively, and χ the iteration number.

We fixed the membrane potential at the value –70 mV and L at 500. Fig. 3 shows the membrane conductance (g_m) for four open probability (P_K) and different open probabilities: (P_{Ca} and P_{Na}).

We notice that for $P_K = 0.1$ and 0.15, the membrane conductance changes quickly from value 0 to 20 pS/cm²
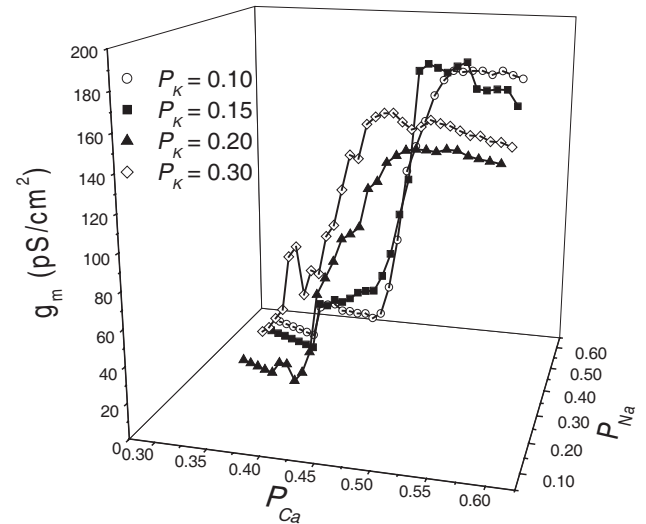
Figure 3. Variation of the membrane conductance (g_m) according to the probabilities P_K, P_{Na} and P_{Ca}. The percolation threshold is reached when the g_m passes from 0 to 0.1 pS/cm², for $P_K = 0.2$, $P_{Na} = 0.45$ and $P_{Ca} = 0.35$.

A

0 mV

-70 mV

B

C
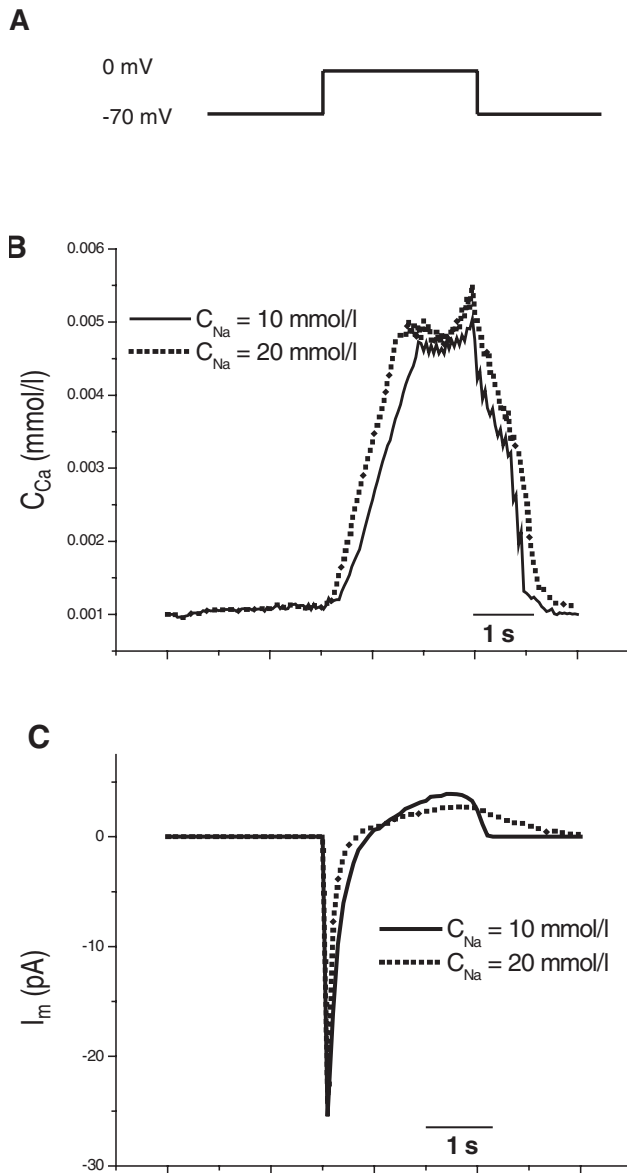
Figure 4. Voltage-clamp simulation. **A.** 3 s depolarisation from −70 to 0 mV. **B.** Variation of the C_{Ca} intracellular concentration. **C.** Compartment of the current membrane for C_{Na} = 10 mmol/l (solid line) and C_{Na} = 20 mmol/l (dot line).

and to 30 pS/cm^2, respectively. For P_K = 0.3, the membrane conductance is non null for all probabilities. These two behaviours do not describe the phase transition in the vicinity of the percolation threshold (Stauffer and Aharony 1991). On the other hand, for P_K = 0.2, the membrane conductance passes from 0 to 0.1 pS/cm^2 with P_{Ca} = 0.35 and P_{Na} = 0.45, this is the percolation threshold of our modelisation. The network is composed of 20% K$_{Ca}$, 35% Ca$_v$ and 45% Na$_v$ channels.

Voltage clamp technique

In this part, we studied the variation of the intracellular Ca^{2+} concentration and the membrane current (I_m) resulting from a 3 s depolarization to 0 mV from a holding potential of −70 mV (Fig. 4), and for two intracellular sodium concentrations 10 and 20 mmol/l.

We notice on Fig. 4B that the depolarizing voltage from −70 mV increases the C_{Ca}, reflecting Ca entry through Ca$_{v-L}$ (L-type Ca channel) and NCX (we did not take into account the plasma membrane Ca^{2+}-ATPase pump function). The exchanger has a stoichiometry of 3 Na$^+$ for 1 Ca^{2+}, is electrogenic and displays a reversal potential at −20 and −40 mV for C_{Na} equal to 10 and 20 mmol/l, respectively (Herchuelz et al. 2002), so that V_m is greater than reversal potential and favors Ca^{2+} entry (outward NCX current). Repolarization promotes Ca^{2+} removal by the exchanger, so that C_{Ca} decreases when V_m becomes more negative (inward NCX current). The simulation shows that elevated concentrations of cytosolic Na$^+$ induce a mode of activity that no longer requires allosteric Ca^{2+} activation (Condrescu and Reeves 2006; Urbanczyk et al. 2006). We announce that high C_{Na} (inhibition of the Na/K pump) (Despa et al. 2002) reduces the Ca^{2+} extrusion through NCX. The C_{Ca} oscillation at repolarisation is due to the balance between an outward and an inward NCX current (Weber et al. 2003).

The membrane current in Fig. 4C highlights the presence of the Na/Ca exchanger. We notice that during the depolarization, the peak inward current is shorter in 20 than in 10 mmol/l intracellular Na$^+$ because of the increased outward NCX current (Zhou and Lipsius 1993; McCarron et al. 1994). During the depolarization, the outward current is smaller in 20 than in 10 mmol/l Na$^+$, because of the inactivation of the Ca^{2+} current (Findlay et al. 2008). What is important is that at repolarization, the outward tail current is larger in 20 than in 10 mmol/l Na$^+$, due to the activation of the K$_{Ca}$ current, resulting from the increased C_{Ca}.

Current clamp technique

We imposed I_m = 10 pA in order to have a resting potential of −70 mV and we modelised the change in membrane potential for two concentrations of Na$_v$: 10 and 20 mmol/l.

For the two intracellular Na$^+$ concentrations, we note a periodic electrical activity, the active phases are named "bursting" (Fig. 5). The burst duration is reduced when the C_{Na} decreased. The shorter burst duration led to a reduction of the Ca^{2+} influx (Sherman et al. 1988; Sherman and Rinzel 1991). A hyperpolarization of 3.08 mV and of 6.7 mV is announced for 10 and 20 mmol/l intracellular Na$^+$ concentrations. This is in agreement with the previous results of the
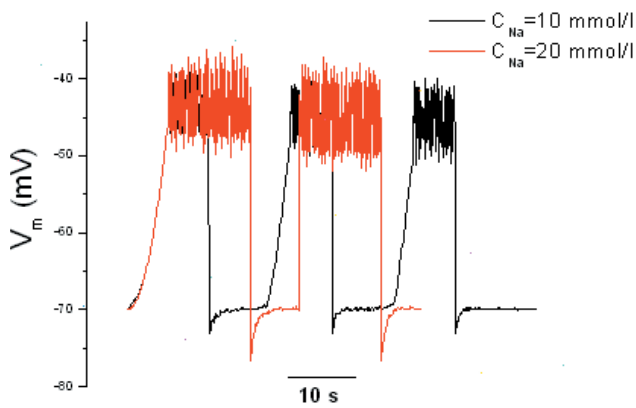
Figure 5. Comparison of burst of membrane potential for two intracellular Na$^+$ concentrations: C_{Na} = 10 mmol/l (in black) and C_{Na} = 20 mmol/l (in red), with a post-hyperpolarisation of 3.08 and 6.7 mV, respectively.

voltage clamp technique; the hyperpolarizing K$^+$ current is more important when C_{Na} increases (Lee et al. 2002). For potentials higher than –45 mV, we observed a repetitive bursting activity due to the spontaneously active channels (Reboreda et al. 2003).

*Distribution of the active channels*

Since it is interesting to follow the evolution of the ion transfer through the plasma membrane, we studied the distribution of the active channels. For that, we represented the network structures of size 100 × 100 for various ion concentrations (Fig. 6).

The K$_{Ca}$ active channels are located in blue, the Na$_v$ active channels in green and the Ca$_v$ active channels in red.

We notice that for the Fig. 6, the concentrations in K$_{Ca}$ are distributed on the four edges of the network that is in good

▶
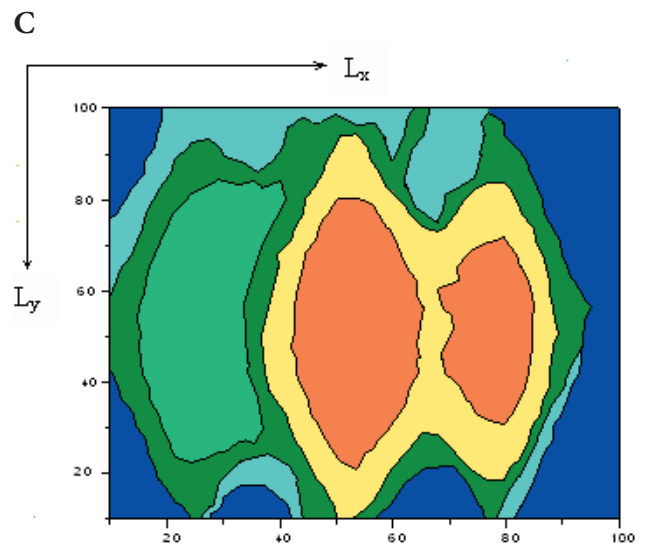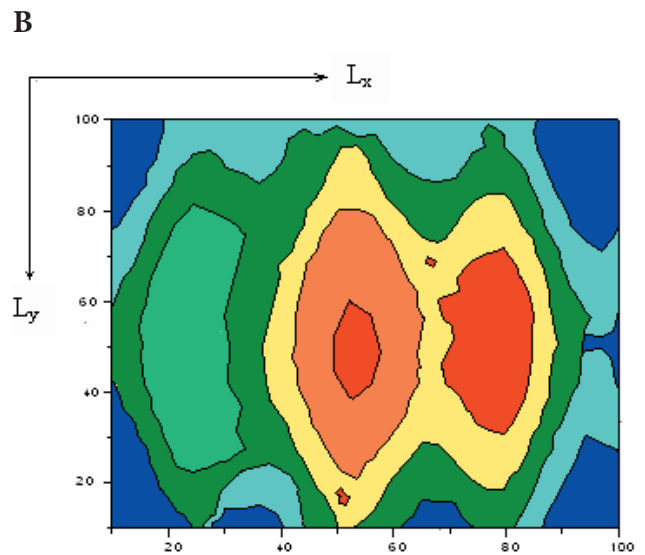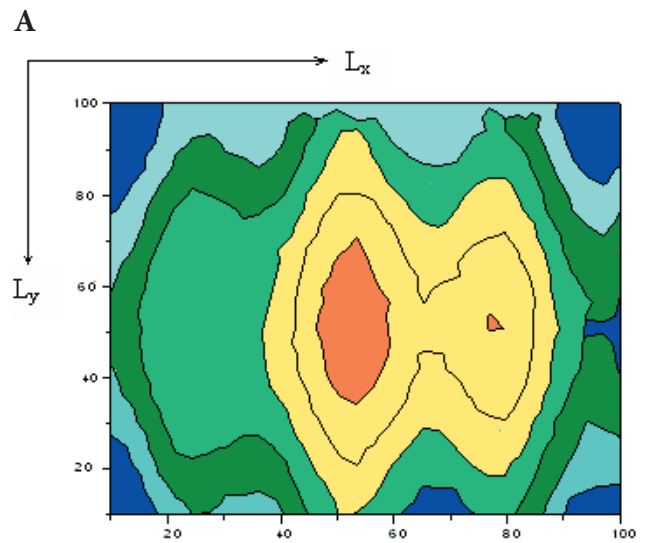
Figure 6. Temporal distribution of the active channels for a network 100 × 100 with various ion concentrations. For the same ion, the colour is in range to indicate the areas moreover at least concentrated. The K$_{Ca}$ active channels are located in blue, the Na$_v$ active channels in green and the Ca$_v$ active channels in red. t = 4, 5, 6 s (A, B, C, respectively).
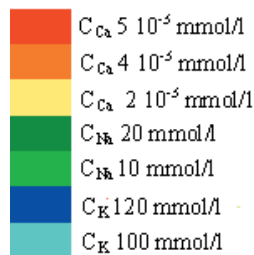
agreement with the FDM conditions. By exploring the three figures, we see that the concentration C_{Ca} increases from 2 to 5 µmol/l in one second. This corresponds to a massive entry of Ca^{2+} ions. Then C_{Ca} returns to its basal concentration at $t = 6$ s, characterised by an efflux of Ca^{2+} ions.

Conclusion

By a simple electric model of the plasma membrane and by a theoretical approach based on the FDM and the percolation concept, we studied the role of the NCX in the regulation of the intracellular Ca^{2+} concentration and the membrane potential oscillations. It should be announced that the NCX and the plasma membrane Ca^{2+}-ATPase pump are two concurrent mechanisms for Ca^{2+} extrusion from the cell.

We detected the presence of an inward current, which is proportional to the intracellular Na^+ concentration and an outward tail current due to the exit of K^+ ions, which causes the hyperpolarization of the plasma membrane. The bursting duration is modified according to the Na^+ intracellular concentration. Large activation corresponds to high C_{Na}. Temporal fractal structures of the active channel distributions enabled us to follow the diffusion of the Ca^{2+} intracellular ions. We compared these results with those of Espinosa Leon (Chouabe et al. 1997) and Zhengyi Wang (Wang et al. 2001) for the study of cardiac hypertrophy and David Gall (Gall et al. 1999) on the pancreatic β-cell. These works showed that the NCX is well implied in the lengthening of the action potential. The combination of the percolation and the FDM gave results in perfect agreement with the experimental results.

References

Bano D., Young K. W., Guerin C. J., Lefeuvre R., Rothwell N. J., Naldini L., Rizzuto R., Carafoli E., Nicotera P. (2005): Cleavage of the plasma membrane Na/Ca exchanger in excitotoxicity. Cell **120**, 275–285

Barg S., Ma X., Eliasson L., Galvanovskis J., Göpel S. O., Obermüller S., Platzer J., Renström E., Trus M., Atlas D., Striessnig J., Rorsman P. (2001): Fast exocytosis with few Ca^{2+} channels in insulin-secreting mouse pancreatic β cells. Biophys. J. **81**, 3308–3323

Bergamini J. F., Aeiyach S., Chane-Ching K. I., Jouini M., Lacroix J. C., Lacaze P. C. (1998): An electrochemical pump: active diffusion across a polypyrrole membrane. J. Chim. Phys. **95**, 1498–1501

Bers D. M, Bassani J. W., Bassani R. A. (1996): Na-Ca exchange and Ca fluxes during contraction and relaxation in mammalian ventricular muscle. Ann. N. Y. Acad. Sci. **779**, 430–442

Blaustein M. P., Lederer W. J. (1999): Sodium/calcium exchange: its physiological implications. Physiol. Rev. **79,** 763–854

Boda D., Varga T., Henderson D., Busath D., Nonner W., Gillespie D., Eisenberg B. (2004): Monte Carlo simulation study of a system with a dielectric boundary: application to calcium channel selectivity. Mol. Simul. **30**, 89–96

Chouabe C., Espinosa L., Megas P., Chakir A., Rougier O., Freminet A., Bonvallet R. (1997): Reduction of $I_{Ca,L}$ and I_{to1} density in hypertrophied right ventricular cells by simulated high altitude in adult rats. J. Mol. Cell. Cardiol. **29**, 193–206

Condrescu M., Reeves J. (2006): Actin-dependent regulation of the cardiac Na/Ca exchanger. Am. J. Physiol. **290**, 691–701

Dallas M. L., Morris N. P., Lewis D. I., Deuchars S. A., Deuchars J. (2008): Voltage-gated potassium currents within the dorsal vagal nucleus: Inhibition by BDS toxin. Brain Res. **1189**, 51–57

Despa S., Islam M. A, Weber C. R., Pogwizd S. M., Bers D. M. (2002): Intracellular Na^+ concentration is elevated in heart failure but Na/K pump function is unchanged. Circulation **105**, 2543–2548

El Makrini M., Jourdain B., Lelièvre T. (2007): Diffusion Monte Carlo method: numerical analysis in a simple case. ESAIM: M2AN **41**, 189–213

Elbasiouny S. M., Bennett D. J., Mushahwar V. K. (2005): Simulation of dendritic $Ca_V1.3$ channels in cat lumbar motoneurons; spatial distribution. J. Neurophysiol. **94**, 3961–3974

Ermentrout B. (2003): Dynamical consequences of fast-rising, slow-decaying synapses in neuronal networks. Neural Comput. **15**, 2483–2522

Faber G. M., Silva J., Livshitz L., Rudy Y. (2007): Kinetic properties of the cardiac L-type Ca^{2+} channel and its role in myocyte electrophysiology: a theoretical investigation. Biophys. J. **92**, 1522–1543

Findlay I., Suzukib S., Murakami S., Kurachi Y. (2008): Physiological modulation of voltage-dependent inactivation in the cardiac muscle L-type calcium channel: A modelling study. Prog. Biophys. Mol. Biol. **96**, 482–498

Flynn G. L., Yalkowsky S. H., Roseman T. J. (1974): Mass transport phenomena and models; theoretical concepts. J. Pharm. Sci. **63**, 479–510

Flynn C. P. (1972): Point defects and diffusion. Clarendon Press, Oxford, England

Gall D., Gromada J., Susa I., Rorsman P., Herchuelz A., Bokvist K. (1999): Significance of Na/Ca exchange for Ca^{2+} buffering and electrical activity in mouse pancreatic β-cells. Biophys. J. **76**, 2018–2028

Garrido J., Mafé S., Pellicer J. (1985): Generalization of a finite-difference numerical method for the steady state and transient solution of the Nernst-Planck flux equations. J. Membr. Sci. **24**, 7–14

Goldman L. (1991): Gating current kinetics in Myxicola giant axons. Order of the back transition rate constants. Biophys. J. **59**, 574–589

González-Caballero F., González-Fernández C. F., Horno J., Hayas A. (1988): On the simulation of nonstationary diffusion through homogeneous membranes using network methods. Z. Phys. Chem. **269,** 1137–1146

Herchuelz A., Diaz-Horta O., van Eylen F. (2002): Na/Ca exchange and Ca^{2+} homeostasis in the pancreatic β-cell. Diabetes Metab. **28**, 3S54–60, discussion 3S108–112

Hilgemann D. W. (1988): Numerical approximations of sodium-calcium exchange. Prog. Biophys. Mol. Biol. **51**, 1–45

Hille B. (2001): Ion Channels of Excitable Membranes. (3rd ed.), Sinauer Associates Inc., U.S.A.

Hodgkin A. L. (1948): The local electric changes associated with repetitive action in a non-medullated axon. J. Physiol. (London) **107**, 165–181

Hodgkin A. L., Huxley A. F. (1952): A quantitative description of membrane current and its application to conduction and excitation in nerve. J. Physiol. (London) **117**, 500–544

Hollerbach U., Chen D.-P., Busath D. D., Eisenberg B. (2000): Predicting function from structure using the Poisson-Nernst-Planck equations: sodium current in the gramicidin A channel. Langmuir **16**, 5509–5514

Hundsdorfer W. H, Verwer J. G. (2003): Numerical Solution of Time-Dependent Advection-Diffusion-Reaction Equations. (Springer Series in Computational Mathematics.) Springer Corp., New York

Ledoux J., Werner M. E., Brayden J. E., Nelson M. T. (2006): Calcium-activated potassium channels and the regulation of vascular tone. Physiology **21**, 69–78

Lee S. H., Kim M. H., Park K. H, Earm Y. E., Ho W. K. (2002): K^+-dependent Na^+/Ca^{2+} exchange is a major Ca^{2+} clearance mechanism in axon terminals of rat neurohypophysis. J. Neurosci. **22**, 6891–6899

Leois R. A., Rae J. L. (1998) : Low-noise patch-clamp techniques. Methods Enzymol. **293**, 218–266

McCarron J. G., Walch J., Fay F. S. (1994): Sodium/calcium exchange regulates cytoplasmic calcium in smooth muscle. Pflügers Arch. **426**, 199–205

Metcalf M., Reid J., Cohen M. (2004): Fortran 95/2003 explainde. (3rd ed.), Oxford University Press

Milescu L. S., Akk G., Sachs F. (2005): Maximum likelihood estimation of ion channel kinetics from macroscopic currents. Biophys. J. **88**, 2494–2515

Miloshevsky G. V., Sizyuk V. A., Partenskii M. B., Hassanein A., Jordan P. C. (2006): Application of finite-difference methods to membrane-mediated protein interactions and to heat and magnetic field diffusion in plasmas. J. Comput. Phys. **212,** 25–51

Morris C., Lecar H. (1981): Voltage oscillations in the barnacle giant muscle fiber. Biophys. J. **35**, 193–213

Morton K. W., Mayers D. F. (1995): Numerical Solution of Partial Differential Equations. Cambridge University Press, New York

Munekazu S. M., Iwamoto T. (2001): Cardiac Na^+/Ca^{2+} exchange: molecular and pharmacological aspects. Circ. Res. **88**, 864–876

Muradoglu M., Tryggvason G. (2008): A front-tracking method for computation of interfacial flows with soluble surfactants. J. Comput. Phys. **227**, 2238–2262

Nonner W., Eisenberg R. (1998): Ion permeation and glutamate residues linked by Poisson-Nernst-Planck theory in L-type calcium channels. Biophys. J. **75**, 1287–1305

Phannkuch H. O. (1963): Contribution a l'étude déplacement de fluides miscibles dans un milieu poreux. Revue de l'Institut Français du Pétrole, No. 2–18

Rappaz M., Bellet M., Deville M. (1998): Modélisation Numérique en Science et Génie des Matériaux (1$^{ère.}$ éd.), Presses Polytechniques et Universitaires Romandes, Lausanne

Reboreda A., Sánchez E., Romero M., Lamas J. A. (2003): Intrinsic spontaneous activity and subthreshold oscillations in neurones of the rat dorsal column nuclei in culture. J. Physiol. (London) **551**, 191–205

Rinzel J., Ermentrout B. (1999): Analysis of neural excitability and oscillations. (Eds. Ch. Koch and I. Segev), pp. 251–292, Chapter 7, MIT Press, Cambridge, Massachusetts

Romero F., Silva B. A., Nouailhetas V. L. A., Aboulafia J. (1998): Activation of Ca^{2+}-activated K^+ (maxi-K^+) channel by angiotensin II in myocytes of the guinea pig ileum. Am. J. Physiol., Cell. Physiol. **274,** 983–991

Rorsman P., Trube G. (1986): Calcium and delayed potassium currents in mouse pancreatic β-cells under voltage-clamp conditions. J. Physiol. (London) **374**, 531–550

Rudy Y., Silva J. R. (2006): Computational biology in the study of cardiac ion channels and cell electrophysiology. Q. Rev. Biophys. **39**, 57–116

Sherman A., Rinzel J. (1991): Model for synchronization of pancreatic β-cells by gap junction coupling. Biophys. J. **59**, 547–559

Sherman A., Rinzel J., Keizer J. (1988): Emergence of organized bursting in clusters of pancreatic a-cells by channel sharing. Biophys. J. **54**, 411–425

Siwy Z., Mercik S., Weron K., Ausloos M. (2001): Application of dwell-time series in studies of long-range correlation in single channel ion transport: analysis of ion current through a big conductance locust potassium channel. Physica A. **297**, 79–96

Stauffer D., Aharony A. (1991): Introduction to Percolation Theory. Taylor and Francis, London

Strikwerda J. C. (1989): Finite Deference Schemes and Partial Deferential Equations. Cole Advanced Books & Software, Pacific Grove, California

Stuart G., Hausser M. (1994): Initiation and spread of sodium action potentials in cerebellar Purkinje cells. Neuron **13**, 703–712

Urbanczyk J., Chernysh O., Condrescu M., Reeves J. P. (2006): Sodium-calcium exchange does not require allosteric calcium activation at high cytosolic sodium concentrations. J. Physiol. (London) **575**, 693–705

Van Eylen F., Albuquerque J., Herchuelz A. (1998): Contribution of Na/Ca exchange to Ca^{2+} outflow and entry in the rat pancreatic β-cell. Diabetes **47,** 1873–1880

Venkataramanan L., Sigworth F. J. (2002): Applying hidden Markov models to the analysis of single ion channel activity. Biophys. J. **82**, 1930–1942

Wakimoto K., Kobayashi K., Kuro-o M., Yao A., Iwamoto T., Yanaka N., Kita S., Nishida A., Azuma S., Toyoda Y., Omori K., Imahie H., Oka T., Kudoh S., Kohmoto O., Yazaki Y., Shigekawa M., Imai Y., Nabeshima Y.-I.,

Komuro I. (2000): Targeted disruption of Na$^+$/Ca^{2+} exchanger gene leads to cardiomyocyte apoptosis and defects in heartbeat. J. Biol. Chem. **275**, 36991–36998

Wang Z., Nolan B., Kutschke W., Hill J. A. (2001): Na$^+$-Ca^{2+} exchanger remodeling in pressure-overload cardiac hypertrophy. J. Biol. Chem. **10**, 1074–1105

Weber C. R., Piacentino V., Houser S. R., Bers D. M. (2003): Dynamic regulation of sodium/calcium exchange function in human heart failure. Circulation **108**, 2224–2229

Zhan X. J., Cox C. L., Rinzel J., Sherman S. M. (1999): Current clamp and modeling studies of low-threshold calcium spikes in cells of the cat's lateral geniculate nucleus. J. Neurophysiol. **81**, 2360–2373

Zhao G., Zhao Y., Pan B., Liu J., Huang X., Zhang X., Cao C., Hou N., Wu C., Zhao K.,Cheng H. (2007): Hypersensitivity of BK$_{Ca}$ to Ca^{2+} sparks underlies hyporeactivity of arterial smooth muscle in shock. Circ. Res. **101,** 493–502

Zhou Z., Lipsius S. L. (1993). Na$^+$-Ca^{2+} exchange current in latent pacemaker cells isolated from cat right atrium. J. Physiol. (London) **466**, 263–285